

High-Mg Lavas in the Karmutsen Flood Basalts, Northern Vancouver Island (NTS 092L): Stratigraphic Setting and Metallogenic Significance

G.T. Nixon, J. Larocque¹, A. Pals¹, J. Styan¹, A.R. Greene² and J.S. Scoates²

KEYWORDS: Vancouver Island, NTS 092L, Wrangellia, Vancouver Group, Karmutsen Formation, stratigraphy, volcanology, metallogeny, flood basalt, high-Mg basalt, picrite, Ni-Cu-PGE

INTRODUCTION

The occurrence of high-Mg lavas in the Triassic Karmutsen flood basalts of the Wrangellia Terrane on northern Vancouver Island has recently been documented by Greene et al. (2006). They identified a number of separate occurrences of high-Mg or picritic pillow lavas and subvolcanic dikes, and designated the excellent exposures of pillowed flows at Keogh Lake as the type locality. Although all currently known picritic basalt flows clearly formed in the submarine environment, their precise stratigraphic position within the Karmutsen Formation has remained uncertain.

The expansion of new logging road systems on northern Vancouver Island over the last decade or so has provided access to more remote areas underlain by Karmutsen volcanic rocks. It is now possible to map distinct stratigraphic subunits within the Karmutsen Formation, similar to those established by earlier workers elsewhere on Vancouver Island. This report, therefore, describes the internal stratigraphy of the Karmutsen Formation, as revealed by recent mapping, and attempts to place known occurrences of high-Mg basalt in the context of this new stratigraphic framework.

The existence of high-Mg basalts in the Karmutsen succession has important ramifications for the mineral potential of this Triassic flood basalt province. Northern Vancouver Island is well known for a number of significant metal prospects and deposits, including intrusion-related Cu-Au-Ag(-Mo) porphyry (e.g., Hushamu, MINFILE 92L 240; the former Island Copper mine, MINFILE 92L 158; MINFILE, 2007); base and precious-metal skarns (e.g., Merry Widow, MINFILE 92L 044); and epithermal precious-metal environments (e.g., Mount McIntosh – Hushamu, MINFILE 92L 240). All such styles of mineralization have strong genetic links to supra-subduction zone metallogenic events associated with the

Late Triassic to Early Jurassic Bonanza magmatic arc (Nixon and Orr, 2007). However, additional exploration opportunities exist in the flood basalt environment, which is known to host world-class magmatic Ni-Cu-PGE deposits associated with high-Mg basalts or their intrusive counterparts.

REGIONAL SETTING

The geology of northern Vancouver Island has been published in a series of 1:50 000 scale maps (Nixon et al., 2006a–d), and revisions to the Early Mesozoic stratigraphy were made recently by Nixon and Orr (2007). A generalized geology map and stratigraphic column for northern Vancouver Island are presented in Figures 1 and 2.

Vancouver Island belongs to the Wrangellia tectonostratigraphic terrane (Jones et al., 1977) of Late Paleozoic to Early Mesozoic rocks, which extends northwards through the Queen Charlotte Islands into southern Alaska (Wheeler and McFeely, 1991). Wrangellia was amalgamated with the Alexander Terrane in the Alaska panhandle to form the Insular Superterrane as early as the Late Carboniferous (Gardner et al., 1988), and was accreted to inboard terranes of the Coast and Intermontane belts as late as the mid-Cretaceous (Monger et al., 1982) or as early as the Middle Jurassic (van der Heyden, 1991; Monger and Journeay, 1994). At the latitude of northern Vancouver Island, Wrangellia is intruded to the east by granitoid rocks of the Coast Plutonic Complex and fault bounded to the west by the Pacific Rim Terrane and metamorphosed and intrusive rocks of the Westcoast Crystalline Complex (Wheeler and McFeely, 1991). Devonian to Early Permian island-arc volcanic, volcanoclastic and sedimentary rocks of the Sicker and Buttle Lake groups (Massey, 1995a–c), which form the basement to Wrangellia, are exposed on southern and central Vancouver Island, and the overlying Middle Triassic shale ('*Daonella* beds') at the base of the Karmutsen is well exposed in the Schoen Lake area, some 30 km southeast of the area shown in Figure 1.

The stratigraphy of northern Vancouver Island is founded upon the Triassic tripartite sequence of Karmutsen flood basalt, Quatsino limestone and Parson Bay mixed carbonate-clastic-volcanic succession, which is diagnostic of Wrangellia (Jones et al., 1977). The occurrence of island-arc volcanic and volcanoclastic strata in the Parson Bay Formation led Nixon and Orr (2007) to take the Parson Bay Formation out of the Vancouver Group and place it in the Late Triassic–Middle Jurassic Bonanza Group. The latter group of volcanic and sedimentary rocks, together with coeval granitoid intrusions of the Island Plutonic Suite,

¹ University of Victoria, Victoria, BC

² University of British Columbia, Vancouver, BC

This publication is also available, free of charge, as colour digital files in Adobe Acrobat® PDF format from the BC Ministry of Energy, Mines and Petroleum Resources website at http://www.em.gov.bc.ca/Mining/GeolSurv/Publications/catalog/cat_fldwk.htm

constitute the main phase of magmatism of the Bonanza island arc (Northcote and Muller, 1972; DeBari et al., 1999).

A major contractional event is marked by an angular unconformity underlying Jurassic–Cretaceous clastic sequences deposited on the eroded surface of the Bonanza

Group. This episode of deformation is constrained by strata of Late Jurassic age (Oxfordian–Tithonian) that locally underlie more widespread Cretaceous sedimentary rocks on northern Vancouver Island and in the Queen Charlotte Islands (Gamba, 1993; Haggart, 1993; Haggart and Carter, 1993).

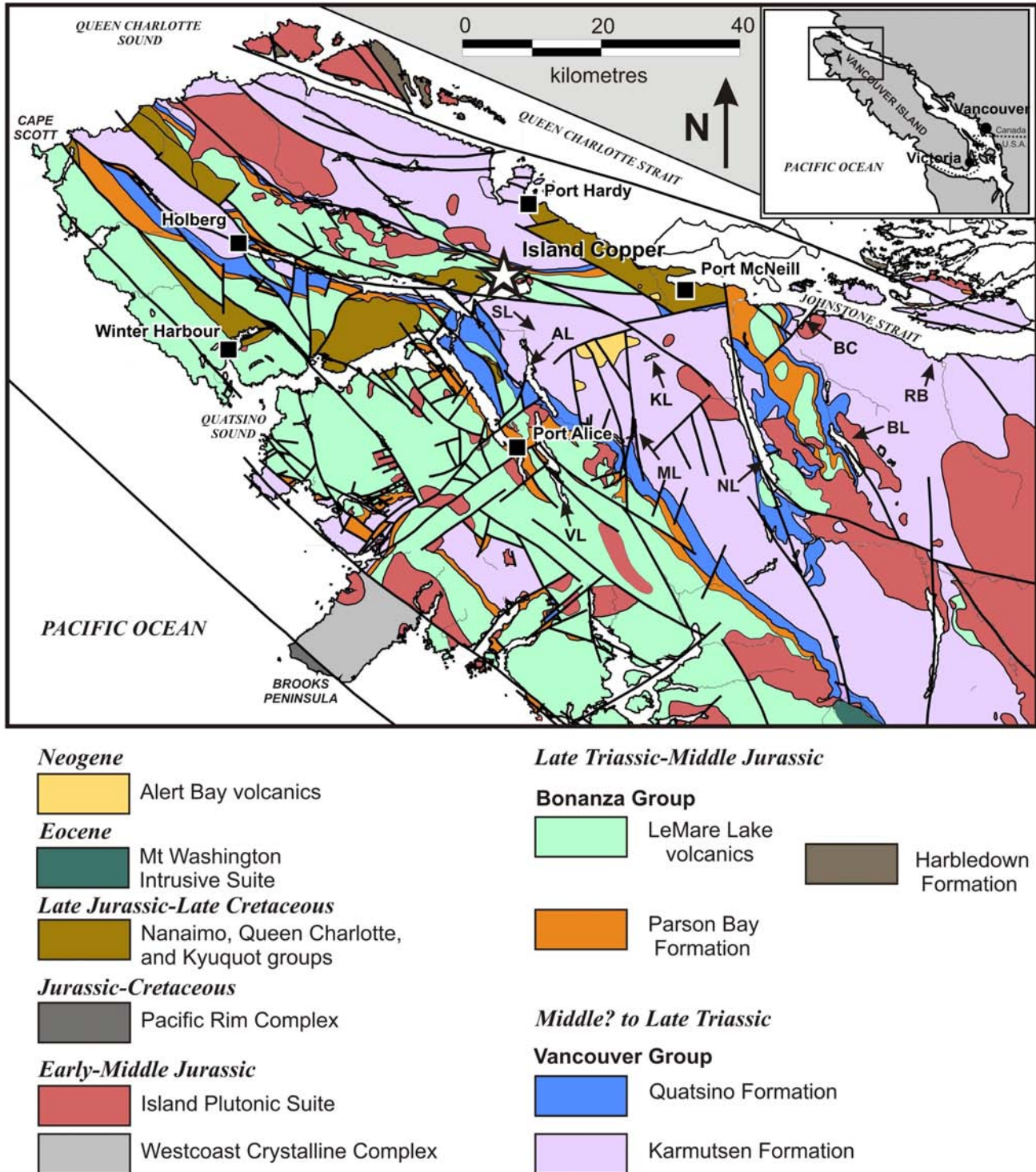


Figure 1. Regional geology of northern Vancouver Island (compiled by Massey et al., 2005). Abbreviations for selected geographic localities: AL, Alice Lake; BC, Beaver Cove; BL, Bonanza Lake; KL, Keogh Lake; ML, Maynard Lake; NL, Nimpkish Lake; RB, Robson Bight; SL, Sara Lake; VL, Victoria Lake.

The history of faulting on northern Vancouver Island is complex and embodies Cretaceous transpression and Tertiary extension. The present crustal architecture exhibits a dominant northwesterly-trending structural grain manifested by the distribution of major lithostratigraphic units and granitoid plutons (Fig 1). Numerous fault-bounded

blocks of homoclinal, Early Mesozoic strata generally dip to the southwest and west (Muller et al., 1974). Jura-Cretaceous clastic strata are preserved as disparate fault-bounded remnants of formerly more extensive Cretaceous basins (Muller et al., 1974; Jeletzky, 1976; Haggart, 1993). The relatively low relief and high heat flow of northern

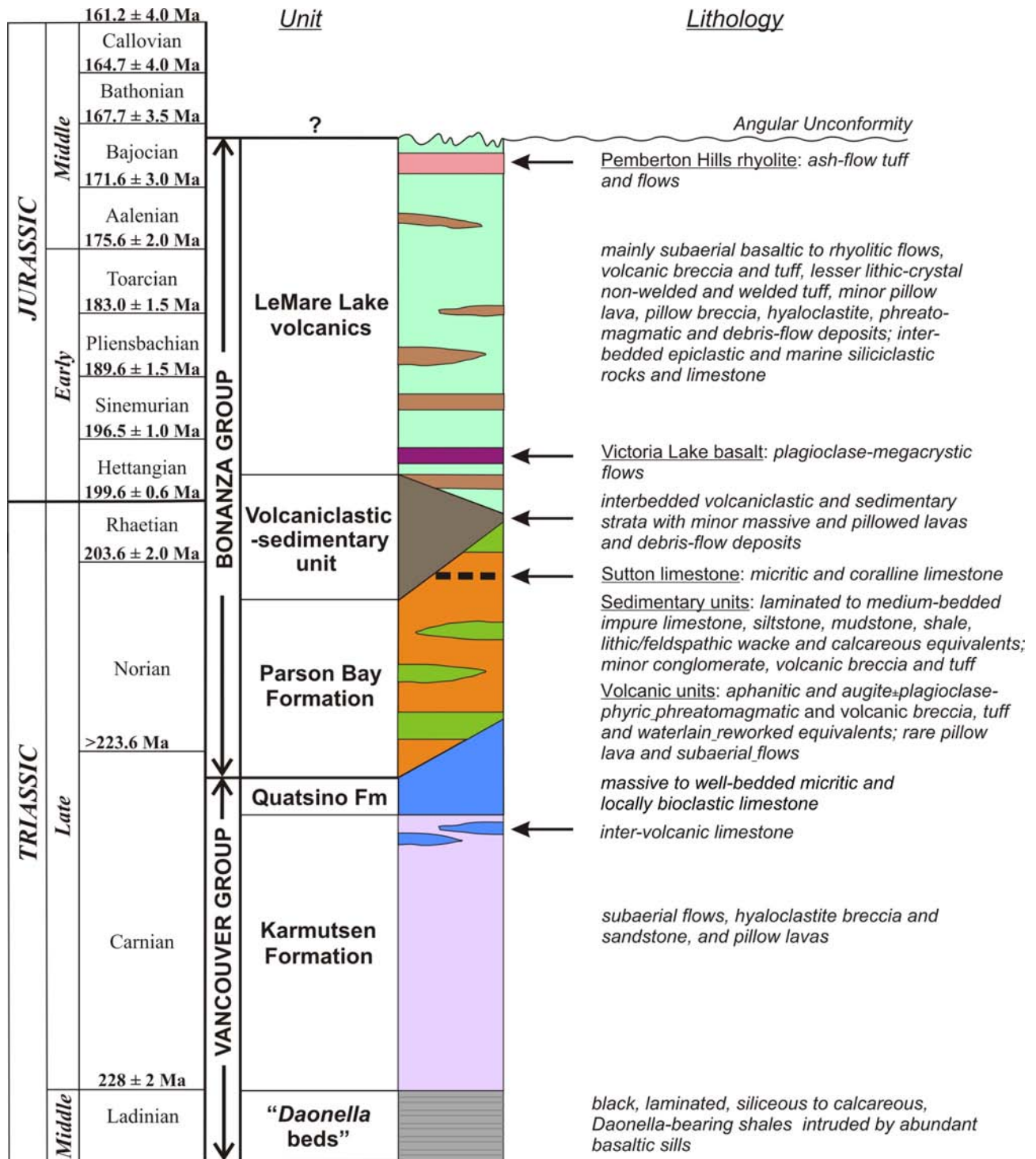


Figure 2. Early Mesozoic stratigraphy of northern Vancouver Island, using the nomenclature for Triassic–Jurassic lithostratigraphic units proposed by Nixon and Orr (2007). The geological time scale is that of Gradstein et al. (2004) except for the Carnian–Norian stage boundary, which is taken from Furin et al. (2006).

Vancouver Island reflect tectonism associated with the development of the Queen Charlotte Basin, a Tertiary transtensional province related to oblique convergence of the Pacific and Juan de Fuca plates with the North American Plate (Riddihough and Hyndman, 1991; Lewis et al., 1997). The distribution of Tertiary volcanic centres appears to be strongly influenced by high-angle faults. The north-easterly-trending Brooks Peninsula fault zone appears to coincide with the southern limit of Neogene volcanism in the region and delineate the southern boundary of the Tertiary extensional regime in the Queen Charlotte Basin (Armstrong et al., 1985; Lewis et al., 1997).

WRANGELLIAN FLOOD BASALTS

The geological setting and evolution of the Triassic flood basalts in the Wrangellia Terrane of northern Vancouver Island was recently reviewed by Greene et al. (2006). The weight of currently available geological evidence indicates that the voluminous ($>10^6$ km³) Wrangellian flood basalts represent an accreted oceanic plateau formed by the rise and demise of a mantle plume (Richards et al., 1991). From fauna and lithostratigraphic correlations, Carlisle and Suzuki (1974) concluded that the Karmutsen basalts range from Middle to Late Triassic (Ladinian–Norian) in age and were emplaced within approximately 2.5 to 3.5 Ma. More recent U-Pb and geochronological studies have so far failed to accurately resolve the age and longevity of Karmutsen volcanism, which is placed at ca. 217 to 233 Ma (see Greene et al., 2006). Despite their age and low (prehnite-pumpellyite) grade of ‘burial’ metamorphism (see Greenwood et al., 1991 and references therein), volcanological and petrographic features of the basalts are typically well preserved, as shown below.

KARMUTSEN FORMATION

The early work of Gunning (1932) established the ‘Karmutsen volcanics’, named for the type area in the Karmutsen Range just west of Nimpkish Lake, as the dominant member of the Vancouver Group. Subsequently, this unit was elevated to formal lithostratigraphic status by Sutherland Brown (1968) and Muller and Carson (1969). The Karmutsen succession in central and northern Vancouver Island was later subdivided by D. Carlisle and coworkers (Carlisle, 1963, 1972; Carlisle and Suzuki, 1974; Muller et al., 1974) into three distinct and mappable volcanic units: 1) closely packed pillow lavas in the lower part of the succession (2900 ± 150 m); 2) pillow breccia and ‘aquagene tuff’ in the middle (610–1070 m); and 3) massive flows at the top (2600 ± 150 m). Intervolcanic sedimentary lenses, principally micritic to bioclastic limestone and black siliceous shale, occur near the top and, less commonly, near the base of the massive flow unit, and are locally associated with pillow lavas, pillow breccias and finer grained, bedded volcanoclastic deposits. The base of the Karmutsen succession overlies a thick (760–920 m) sequence of black siliceous to calcareous shale (‘*Daonella* beds’) of Middle Triassic age, intruded by abundant mafic sills that are considered comagmatic with Karmutsen volcanic rocks (Carlisle, 1972; Carlisle and Suzuki, 1974; Muller et al., 1974). The shale unit is exposed south of the current area of interest near Schoen Lake (see Greene et al., 2006). According to previous work, estimates for the cumulative thickness of the Karmutsen Formation exceed 6000 m.

Yorath et al. (1999) proposed that the excellent exposures along Buttle Lake on central Vancouver Island represent the most complete section.

Recent mapping of the Karmutsen Formation on northern Vancouver Island has resulted in a tripartite division of the volcanic succession (Fig 3–5), analogous to the sub-units originally established by Carlisle (1963, 1972): 1) a pillow lava unit at the base, dominated by closely packed pillowed flows with minor intercalated sheet flows; 2) an overlying hyaloclastite unit characterized by pillow-fragment breccias and fine-grained hyaloclastite deposits, and intercalated locally with pillowed flows throughout the succession; and 3) an upper massive flow unit dominated by subaerial lavas but including minor limestone, fine-grained siliciclastic sedimentary rocks, pillow lavas and volcanoclastic deposits near the top and base. The genetic term ‘hyaloclastite’ has been adopted to denote volcanic rocks formed by quench-fragmentation and autobrecciation during interaction with water, rather than the classic term ‘aquagene tuff’, as originally employed by Carlisle (1963), which may connote an origin via explosive fragmentation and deposition directly by pyroclastic processes (Cas and Wright, 1987). Although certain basaltic shard morphologies described by Carlisle (1963) may have a pyroclastic origin, generated, for example, by steam explosions where lava flows entered the ocean, there is abundant evidence to conclude that the overwhelming majority of volcanoclastic products in the Karmutsen succession are related to the emplacement and granulation of pillowed flows, as well as resedimentation of hyaloclastites in the submarine environment.

Pillow Lava Unit

Pillow lavas in the basal part of the Karmutsen Formation are exposed on the coast north of Robson Bight, and in roadcuts and quarries along logging roads stretching west from the Karmutsen Range to Sara Lake, just west of Twin Peaks (Fig 3). The base of the pillow lava unit is typically cut off by faulting and is not exposed in the map area. The top of the unit appears broadly conformable with overlying beds of hyaloclastite, and map patterns northwest of Maynard Lake indicate interdigitation of pillows and the basal part of the hyaloclastite unit. The minimum thickness of the pillow lava sequence, as estimated in a coastal section between Beaver Cove and Robson Bight, is approximately 3000 m, assuming no significant repetition by faults.

Dark grey to grey-green pillows generally exhibit nearly equidimensional to lobate forms up to about 1.5 m in length and 1 m across, and typically are closely packed with very dark grey to black, well-chilled, chlorite-rich selvages (Fig 6A). The majority of the pillow sequence is aphanitic, nonamygdaloidal and strongly to nonmagnetic. However, towards the top of the succession, pillow lavas may carry plagioclase phenocrysts and exhibit amygdaloidal textures. Individual pillows may display pronounced radial jointing, but this is not a common feature. Interstices are commonly devoid of clastic material, or may host subequant to rectangular or distinctly elongate, curvilinear shards that represent the spalled rims of pillows (Fig 6B). This material is commonly partly altered to chlorite, epidote, quartz and carbonate, for which the local term ‘dallasite’ has been coined. Complete replacement or infilling of interstices and irregular fractures by quartz, chlorite, epidote, calcite, potassium feldspar and zeolite usually aids in identifying pil-

low morphologies in blasted outcrops. Rarely, large pillows in cross-section exhibit quartz-filled ledges with flat floors and convex roofs, interpreted to represent cavities evacuated by lava during emplacement (i.e., small lava tubes). These drainage channels provide valuable structural indicators for way-up, flow orientation and flow contacts (bedding). Such features may occur as stacked lava tubes within a single pillow, and have been described previously (e.g., Yorath et al., 1999, Fig 46).

Pockets of pillow breccia and rare, laminated to thinly bedded hyaloclastite sandstone and massive sheet flows are encountered locally throughout the succession. The sheet flows may be more common than appreciated due to the scarcity of well-exposed contacts and similarity of their textures to subvolcanic dikes and sills. The best exposures of sheet flows occur in quarries and high roadcuts (Fig 6C). The convolute nature of their lower contact, which is typically draped over underlying pillows, serves to distinguish the sheet flows from subvolcanic intrusions (Fig 6D). Although most sheet flows lack internal structures, some exhibit a crude curvilinear jointing oriented at a high angle to their contacts. The occurrence of sheet flows deep within the pillow basalt succession, and their generally nonamygdaloidal nature, indicates that they are truly submarine in origin rather than the result of sea-level oscillation between submarine and subaerial conditions. Most appear to have lensoid geometry and likely reflect a local increase in the flow rate relative to the rate of emplacement of pillows.

In thin section, basaltic pillow lavas are weakly to nonamygdaloidal, and aphyric or porphyritic with small amounts of plagioclase and/or olivine phenocrysts. Plagioclase-bearing and/or amygdaloidal lavas begin to appear near the top of the pillow lava succession. Euhedral to subhedral plagioclase and olivine phenocrysts (<2 mm) may form glomerophytic clots, and groundmass plagioclase generally forms acicular crystals. Olivine is completely replaced by fine-grained intergrowths of serpentine, chlorite, carbonate, opaque oxides and/or quartz. In aphyric pillow lavas, clinopyroxene usually forms radiating dendritic to sheaf-like crystals with a variolitic texture, or intergranular microphenocrysts. In porphyritic lavas, clinopyroxene is typically somewhat coarser grained and exhibits a prismatic or ophitic habit.

Hyaloclastite Unit

The hyaloclastite unit crops out on the coast between Beaver Cove and Robson Bight, and can be traced westward through well-forested ground extending from the west flank of the Karmutsen Range to Sara Lake (Fig 3). Where adequate structural control is present, the upper and lower contacts of this unit appear conformable with overlying flow and underlying pillow sequences. The thickness of this unit varies considerably across the map area. It attains an estimated maximum thickness of approximately 1550 ±200 m in a coastal section north of Robson Bight, and may be less than 40 m thick in the Maynard Lake area.

Excellent exposures of the hyaloclastite unit are found along the coast south of Beaver Cove (Fig 3). Massive to thickly bedded volcanic breccia is the dominant lithology, interbedded with subordinate, well-bedded basaltic sandstone and lesser amounts of pillow lava. The relationships between all three rock types and their inherent textural characteristics are well illustrated in the coastal section. At

one locality, for example, dark greenish grey, closely packed pillow lavas are succeeded upward by sandstones and volcanic breccias, and textures and a wealth of sedimentary structures elucidate the origin and mode of deposition of the volcanoclastic rocks (Fig 7). The lowermost pillows (<1 m in length) are aphanitic and nonamygdaloidal, and have locally trapped laminated and deformed sediment in their interstices during emplacement (Fig 7A). The pillows are overlain by pale buff to dark grey-green weathering, thinly laminated to medium-bedded, medium to coarse-grained sandstone composed predominantly of angular to subangular basaltic shards of hyaloclastite origin. The thicker beds of hyaloclastite sandstone may enclose angular to subrounded clasts of basalt (<8 cm across), some of which preserve chilled pillow rinds, whereas laminated horizons may display crossbedding and spectacular slump folds and fluidization structures (Fig 7B, C). At the locality illustrated, slumped beds lie directly beneath a very thick bed of dark grey-green hyaloclastite breccia containing sparse pillow fragments and rare whole pillows, up to 1.5 m in length, set in a finely comminuted sand-size matrix of granulated hyaloclastite material. The clasts are generally matrix supported and poorly sorted. Many clasts are not obviously derived from pillow rims and probably represent fragmented pillow cores. Elsewhere, pillow-fragment breccias are more easily recognized due to the abundance of clasts of broken and whole pillows (Fig 7D). The lower contact of the underlying disturbed-bedding horizon (Fig 7B) is marked by a fairly sharp discontinuity, whereas the upper contact is transitional into the matrix of the breccia bed. Graded bedding is evident in some of the thin sandstone beds, and crude normal grading may be rarely recognized in some of the breccia layers. From these well-preserved sedimentary features, it is clear that the coarse volcanic breccias were emplaced via debris flows carrying unconsolidated hyaloclastite material downslope, thereby causing rapid loading and dewatering, and localized detachment, of semiconsolidated hyaloclastite sandstone deposited previously by turbidity currents.

In thin section, the hyaloclastite sandstone and the breccia matrices are rich in dark brown, angular to subangular, subequant to highly elongate shards of palagonitized and devitrified, pseudo-isotropic basaltic glass, representing the resedimented quench-fragmentation products of pillow lava (Fig 8). Finely comminuted matrices are generally pervasively altered to a fine-grained mixture of chlorite, quartz and prehnite, along with minor epidote, carbonate and iron oxide. The rims of shards and clasts are commonly bleached and/or marked by concentrations of finely crystalline opaque material, and some fragments preserve whole or partial vesicles usually infilled by secondary minerals. Broken plagioclase crystals occur in some matrices, and larger clasts may enclose euhedral to subhedral plagioclase phenocrysts (Fig 8B).

Massive Flow Unit

A thick sequence of subaerial flows caps the lava pile and forms the most aerially extensive map unit in the Karmutsen Formation of northern Vancouver Island. The lower contact with the hyaloclastite unit is essentially conformable (local, irresolvable disconformities probably exist), and flows generally rest on pillow-fragment breccia or pillow lava locally present at the top of the hyaloclastite succession. At some localities, pillow-like morphologies scattered within more massive flows may mark a transition

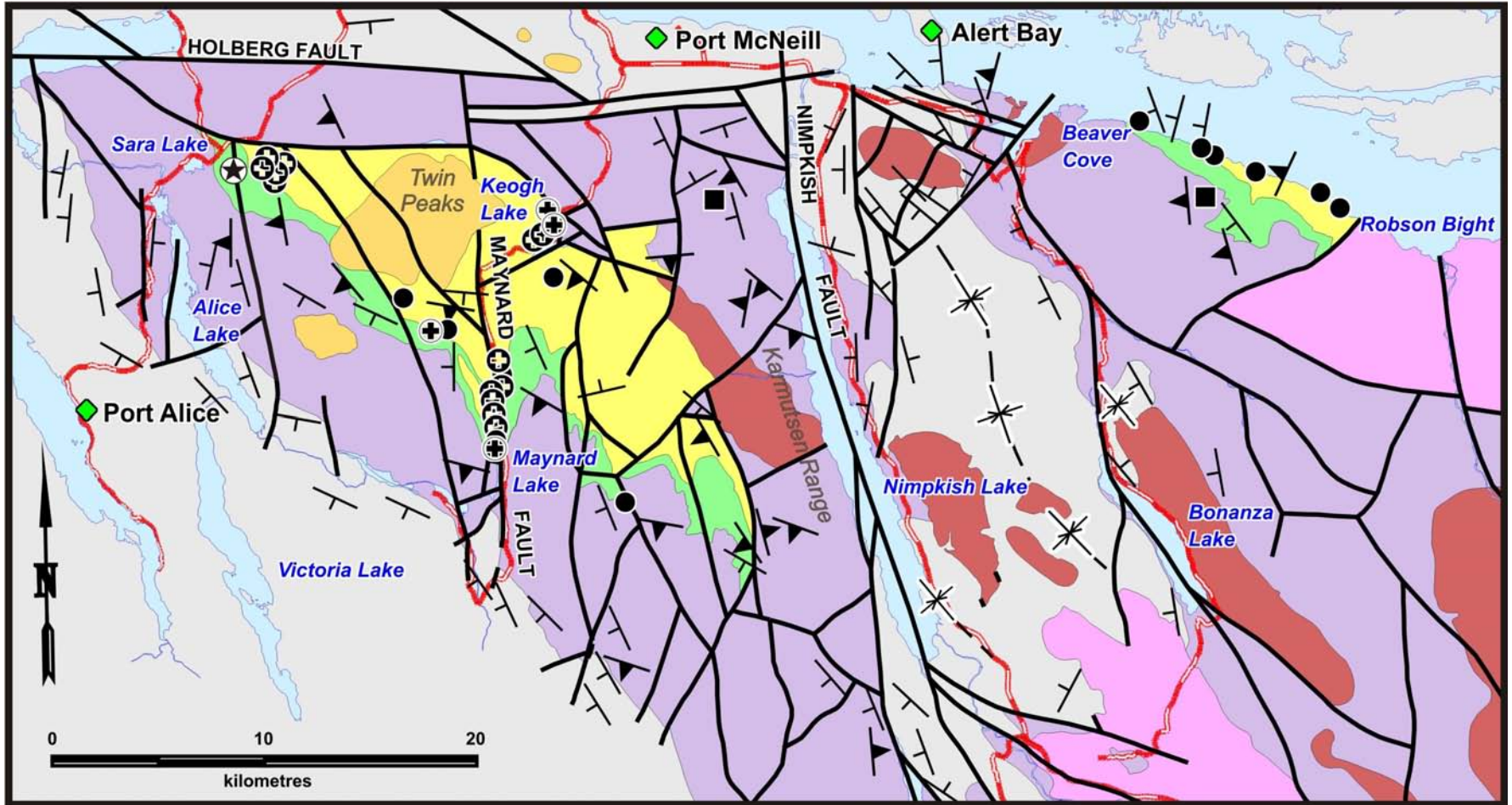


Figure 3. Generalized geology of the Late Triassic Karmutsen Formation in the Port Alice – Port McNeill – Robson Bight area, showing the location of olivine-bearing and high-Mg basalts in relation to the distribution of massive flow, hyaloclastite and pillow lava sequences. Other map units are undifferentiated (grey), except for the Tertiary Alert Bay volcanic rocks and intrusions of the Island Plutonic Suite (see Fig 1).

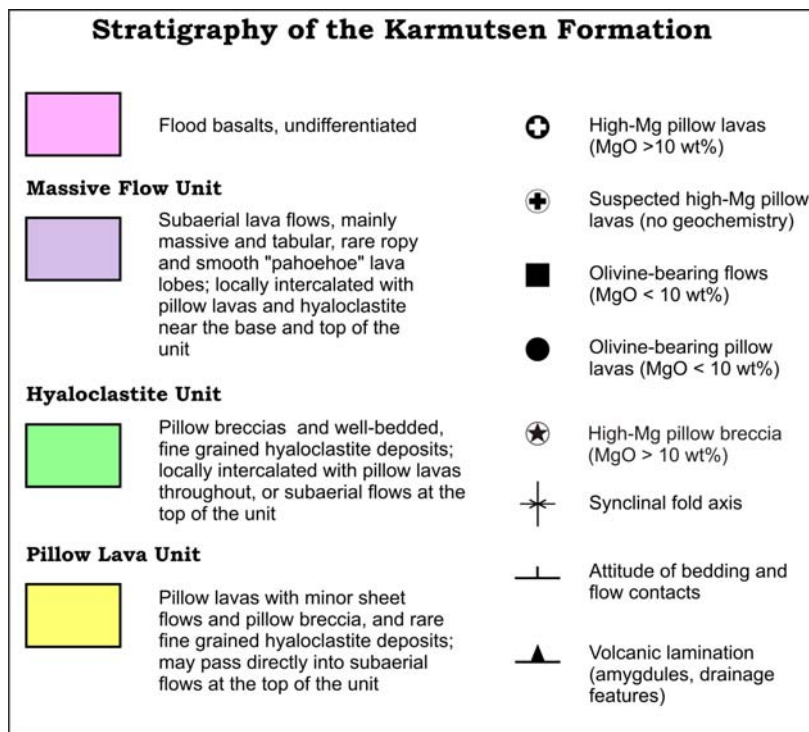


Figure 4. Legend for the geology map of the Karmutsen Formation (Fig 3, opposite).

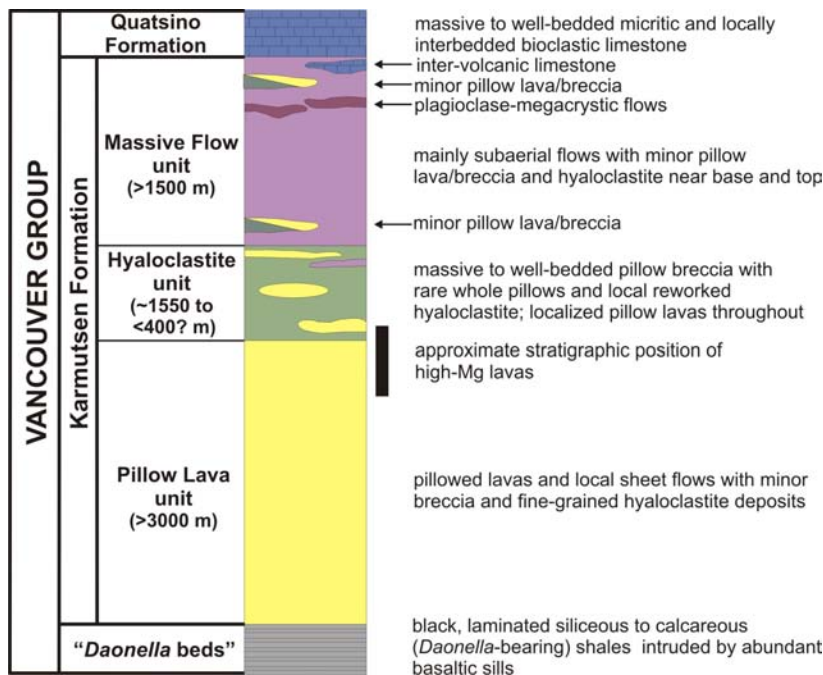


Figure 5. Stratigraphy of the Karmutsen Formation, showing the tripartite subdivision into basal pillow lavas, overlying hyaloclastite deposits and younger massive flow units. Note that known occurrences of high-Mg basalt appear to lie near the top of the pillow lava sequence.

from submarine to subaerial effusive volcanism. At the upper contact, Quatsino limestone rests directly on the flows, or is separated from them by a thin (<1 m) layer of calcareous basaltic sandstone and siltstone representing the water-laid weathering products of the lava shield. The uppermost

part of the flow sequence has a distinctive stratigraphy that includes thin (typically <6 m thick and rarely exceeding 15 m) pockets and lenses of pale grey weathering, micritic to bioclastic, and rarely oolitic, intervolcanic limestone, similar to the Quatsino Formation, and rare shale and siltstone. Locally, intra-Karmutsen limestone is associated with thin sequences of pillow lava and hyaloclastite deposits, which may also occur intercalated between the flows. Distinctive megacrystic lavas, charged with blocky to prismatic, euhedral to subhedral plagioclase crystals reaching 1 to 2 cm in length, are restricted to this part of the section (Fig 5). The minimum thickness of the massive flow unit, as estimated from its upper contact with Quatsino limestone to the granitoid intrusion west of Beaver Cove, is approximately 1500 m.

The dark grey to grey-green or dusky red flows are generally aphanitic to fine grained, especially in flow interiors, or plagioclase phyric, and have strongly amygdaloidal to nonamygdaloidal textures and moderate to strong magnetic response. Plagioclase phenocrysts (typically <4 mm) are more common in the upper part of the flow sequence. Plagioclase megacrysts (usually 1–2 cm) occur in basalts near the top of the unit, generally below intra-Karmutsen limestone, and are evenly distributed throughout the flow (10–20 vol% crystals) or locally concentrated in zones with up to 40 to 50 vol% crystals. The megacrysts are generally arranged haphazardly, presumably due to the high viscosity of these crystal-choked layers.

The morphology of the massive flow unit is commonly rendered as ledges protruding from steep hillsides. The unit is composed predominantly of simple flows, generally ranging from about 2 to 6 m thick, although some flows are thinner (<0.5 m) and others appear to exceed 15 m in thickness. Rarely, ropy and smooth 'pahoehoe' lava crusts and lobes in compound flows are well preserved (Fig 9A–C). The contacts between individual flows are typically sharp and planar to curvilinear, and are indistinct in many outcrops. Definitive features marking flow contacts include amygdaloidal flow tops overlain by dense, compact zones at the base of the overriding flow that locally exhibit hackly joint patterns and/or zones of pipe vesicles commonly filled with quartz and zeolites (Fig 9D).

Contacts may exhibit noticeably different degrees of oxidation, as reflected by hematitic alteration, but flow breccia and paleosol development are entirely absent. As noted by Greene et al. (2006), columnar jointing, common in many continental flood basalt provinces, is completely lacking in

Karmutsen flows. Crude columnar jointing, however, has been observed in certain sills. By far the most common internal fabric is a flow lamination marked by amygdule concentrations ranging from several centimetres to (rarely) 0.5 m thick and commonly arranged in parallel layers within the outcrop. This amygdaloidal layering invariably shares the same orientation as flow contacts, where present, and may be used as a valuable structural indicator in the absence of bedding information (Fig 3). Nested drainage channels filled with drusy quartz crystals, identical to those described previously in the basal pillow lava unit, are sparsely distributed yet provide good substitutes for bedding and clear evidence of local flow orientation (Fig 9E, F).

In thin section, the porphyritic flows contain phenocrysts of plagioclase, or both olivine and plagioclase, set in a fine-grained groundmass containing clinopyroxene, plagioclase and opaque oxides. Subhedral to anhedral olivine crystals (<1.5 mm) are found in lavas with as little as 6 wt% MgO (*see below*). Megacrystic flows contain euhedral laths and blocky crystals of calcic plagioclase up to 2 cm in length and exhibit either a serial size gradation towards the groundmass or hialtal textures. Subhedral olivine commonly forms glomerophyric intergrowths with, or inclusions within, plagioclase phenocrysts. Clinopyroxene may be present as intergranular grains, particularly in aphyric flows, or display subophitic to ophitic textures, most prevalent in plagioclase-phyric lavas, especially the

centres of thick flows. Secondary alteration assemblages and amygdule infillings include quartz, epidote, chlorite, zeolite, potassium feldspar and carbonate, and rarely iron oxides, chalcopryrite and native copper.

High-Mg Lavas

The high-Mg lavas are arbitrarily defined as having MgO >10 wt% and, in the geochemical classification described below, are predominantly magnesian basalt and picrite. The principal outcrops are at Keogh Lake, the type locality, and close to Sara Lake in the west and Maynard Lake in the east (Greene et al., 2006). New exposures of high-Mg lavas identified in this study are situated on the eastern side of the Maynard fault (Fig 3). To date, practically all high-Mg lavas are restricted to the basal pillow basalt unit, where they form both pillowed and sheet flows. A subvolcanic dike and pillow-fragment breccia described by Greene et al. (2006, Fig 7, 8) likewise have high-Mg compositions. The stratigraphic position of these high-Mg rocks, as determined in this study, lies close to the top of the basal pillow basalt sequence and within the base of the overlying hyaloclastite unit (Fig 3, 5).

All high-Mg rocks contain variable amounts of olivine phenocrysts, rarely visible in outcrop due to complete replacement by secondary mineral assemblages (*see* Greene et al., 2006, Fig 6, 7). Olivine phenocrysts, typically accompanied by plagioclase, also occur in rocks with

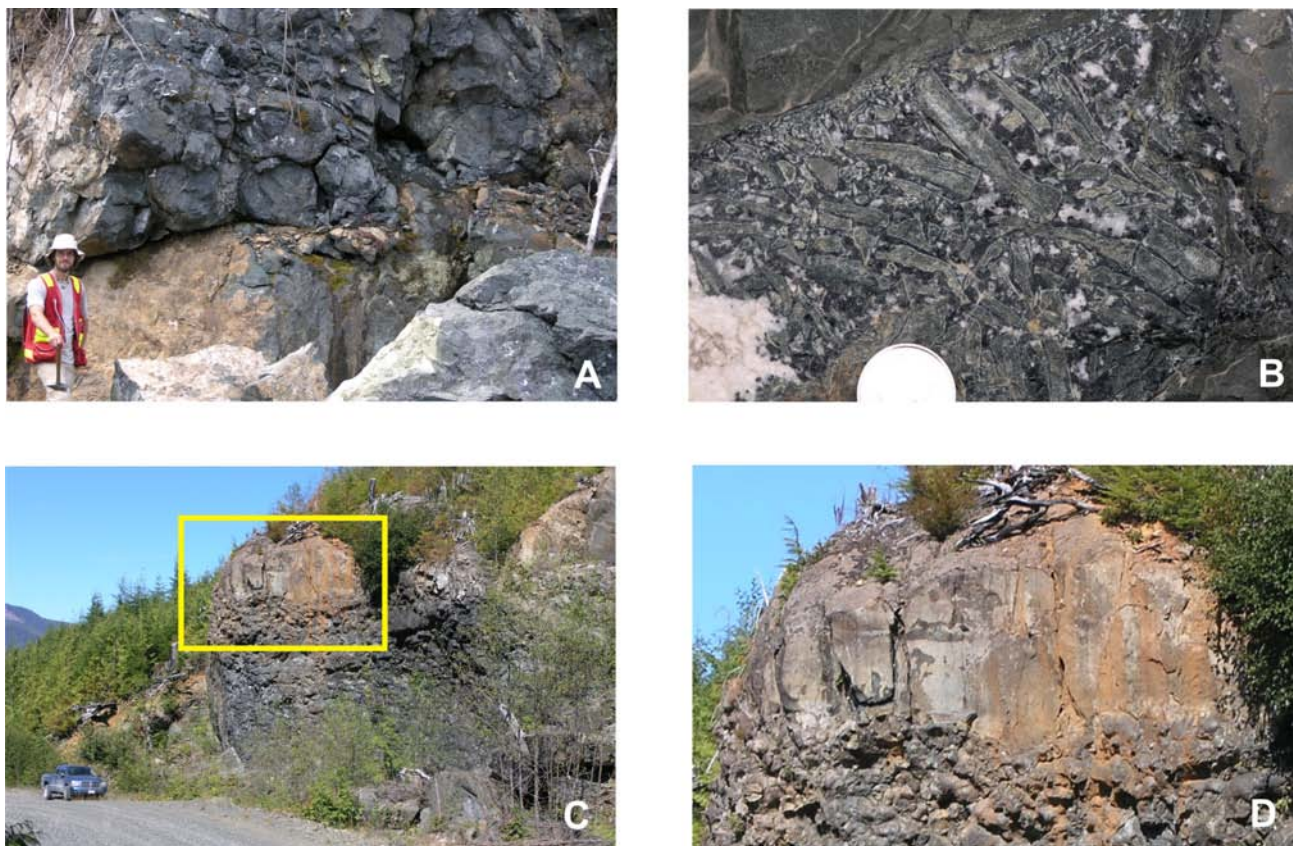


Figure 6. Karmutsen pillow basalt: A) closely packed pillows intercalated with pillow breccias inferred to lie near the top of the massive subaerial flow unit (locality 06GNX3-3-1); B) elongate to curvilinear glassy shards formed from quench-fragmented rinds of tholeiitic pillows in the basal pillow basalt unit, devitrified and altered to chlorite, quartz, epidote and zeolite ('dallasite'); C) localized massive sheet flow intercalated with high-Mg pillow lavas near the top of the pillowed unit (locality 06GNX34-4-1); D) detail of base of sheet flow (inset in C) draped over pillows.

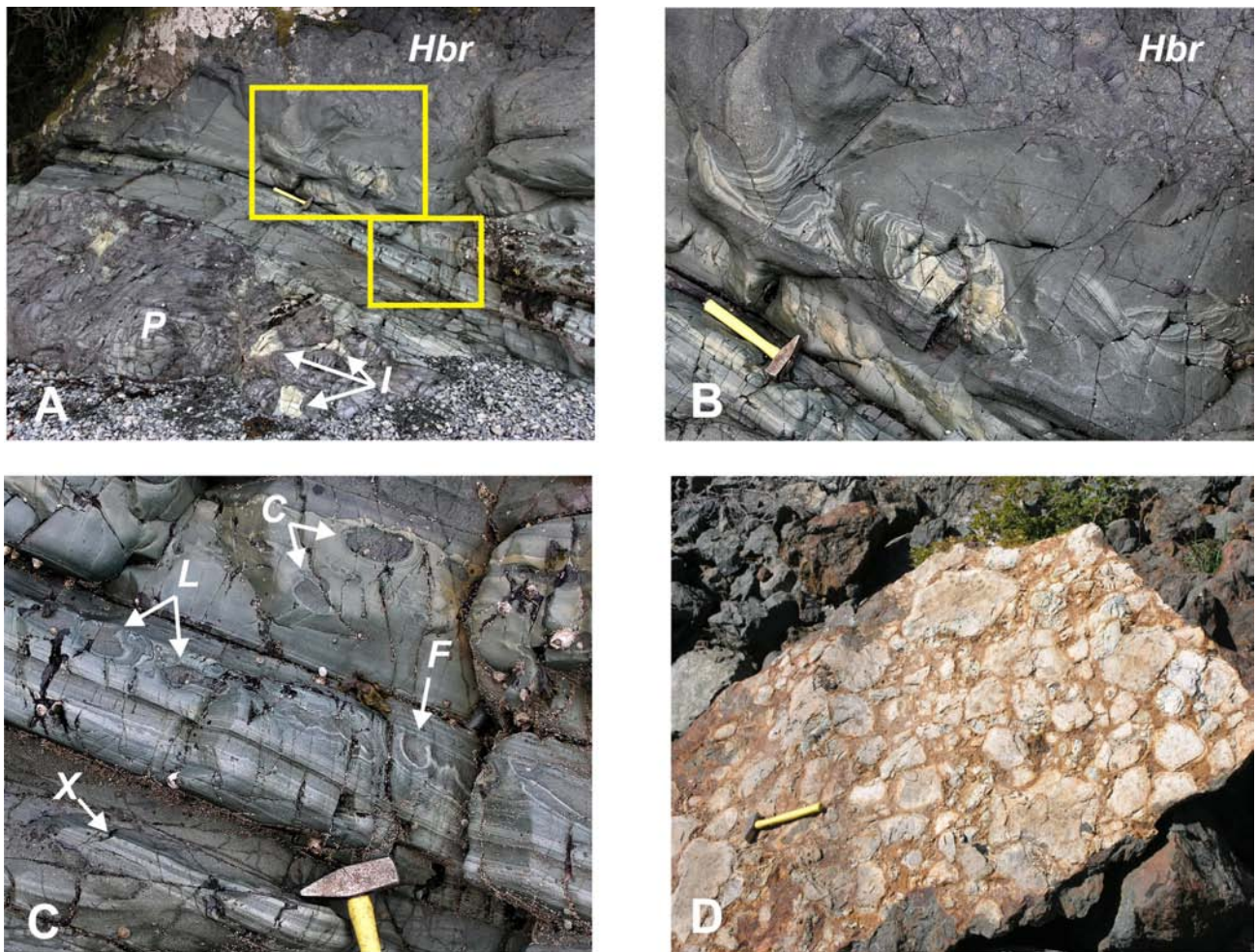


Figure 7. Volcanological and sedimentary features of the hyaloclastite unit: A) intraformational pillow lava (P) with trapped interpillow hyaloclastite sediment (I), overlain by thinly bedded hyaloclastite sandstone exhibiting remobilized bedding near the contact with overlying hyaloclastite breccia (Hbr) rich in broken pillow fragments (locality 07GNX10-5-1); B) slumped and rotated hyaloclastite beds beneath pillow-breccia debris flow (area shown in A); C) well-developed flame structures (F) and load casts (L) in beds below a debris flow that also exhibit crossbeds (X) and contain dispersed basaltic clasts (C; inset shown in A); D) pillow-fragment breccia exhibiting dispersed whole pillows and a rusty, pyritic hyaloclastic matrix (locality 06GNX34-6-1).

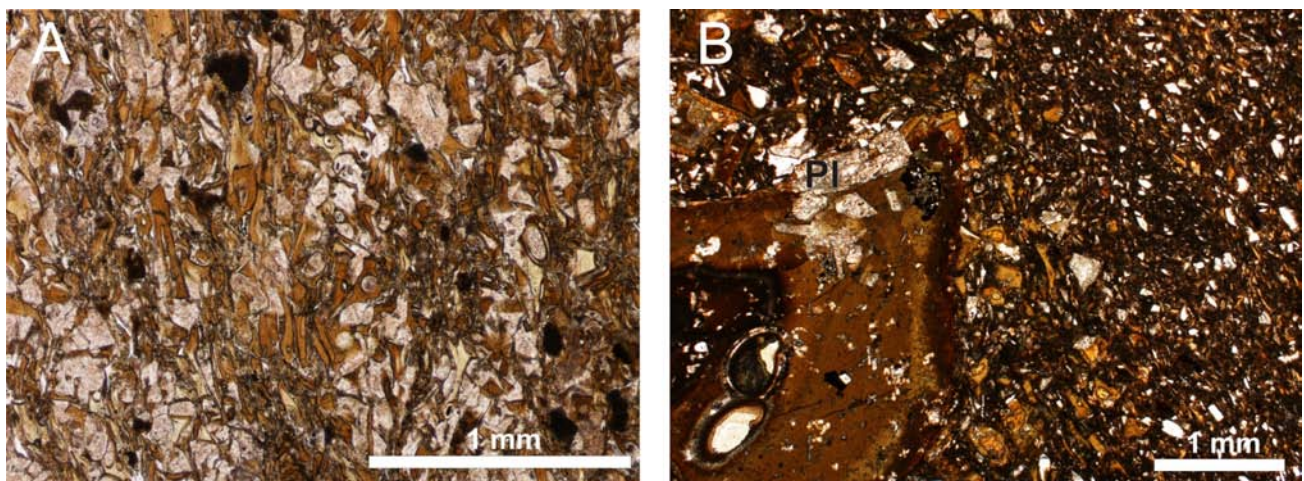


Figure 8. Photomicrographs of hyaloclastite textures: A) dark brown, palagonitized shards of devitrified, pseudo-isotropic basaltic glass and more finely comminuted material in laminated hyaloclastite sandstone, partially replaced and cemented by prehnite (white); B) small angular clast of palagonitized vesicular basalt (lower left) with a partially embedded plagioclase phenocryst (PI) enclosed in hyaloclastite sandstone. Both photomicrographs are of sample 07GNX11-4-1 in plane-polarized transmitted light.

<10 wt% MgO, which appear more widespread (Fig 3). High-Mg lavas are difficult to distinguish from tholeiitic basalt in the field, and positive identification requires geochemical analysis and petrographic observation. The most diagnostic physical property is their generally nonmagnetic

character and extremely low magnetic susceptibility readings.

The dark grey to greenish grey high-Mg pillow lavas are typically closely packed with virtually no interstitial hyaloclastite, and are spatially associated with less

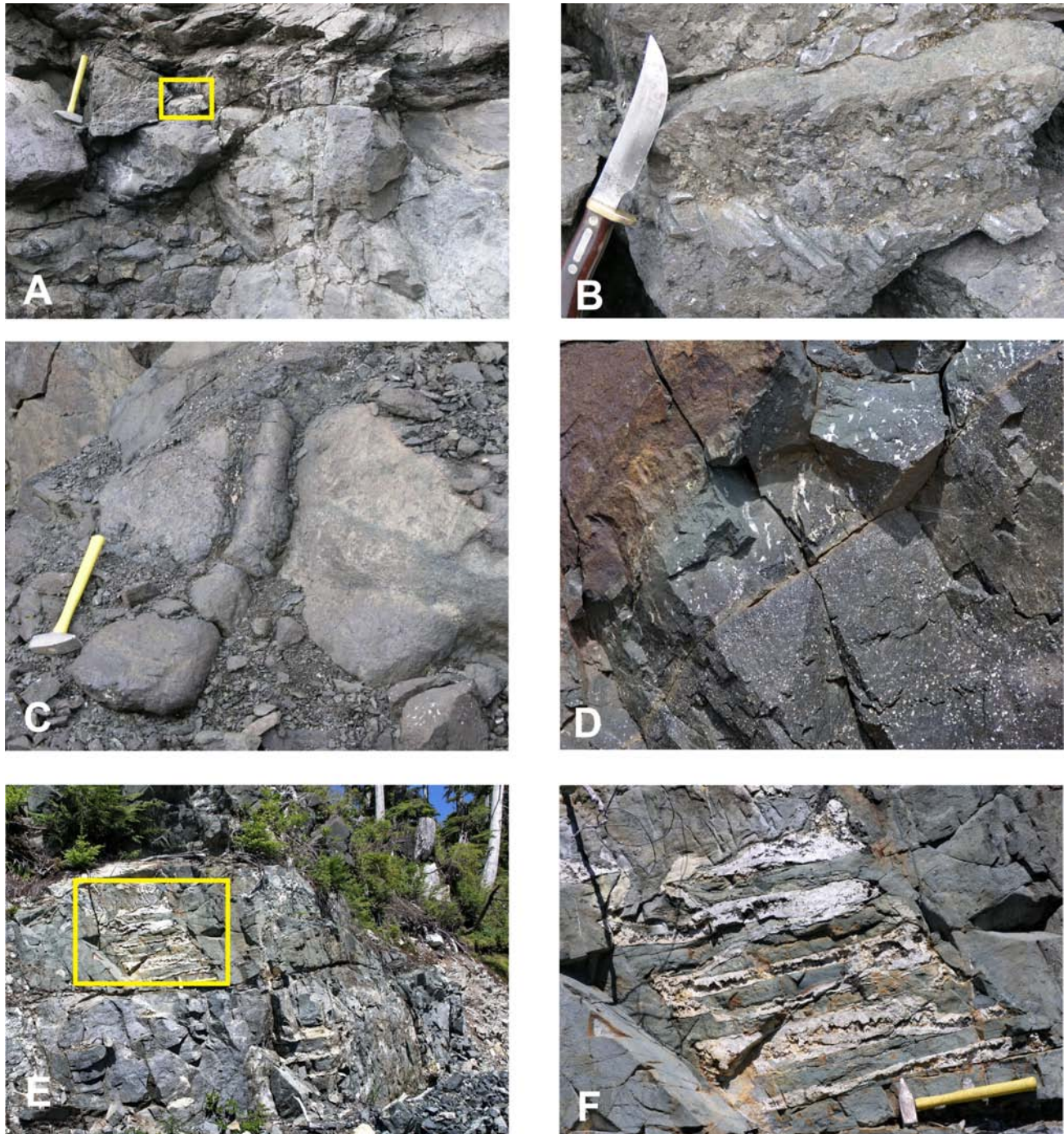


Figure 9. Volcanological features of subaerial Karmutsen basalts: A) cross-section through thin 'pahoehoe' flow lobes with smooth undulatory contacts dipping gently towards camera (locality 06GNX11-5-1); B) close-up of curvilinear, ropy (pahoehoe) lava crust protruding below thin overlying flow (area shown in A); C) smooth pahoehoe flow lobe in the same quarry; D) sharp contact between massive flows, showing amygdule-rich flow top in sharp contact with the dense base of the overlying flow, which exhibits a well-developed zone of pipe vesicles deformed in the direction of flow (left to right; locality 07GNX25-5-1); E) massive flow unit, exhibiting multiple lava drainage ledges (lava tubes) infilled with quartz (locality 07GNX13-5-1); F) close-up of vuggy quartz ledges (area shown in E).



Figure 10. Photomicrograph of high-Mg basalt in a massive sheet flow at the type locality at Keogh Lake. Euhedral to subhedral olivine phenocrysts are set in a groundmass of calcic plagioclase, clinopyroxene and granular opaque oxides. The olivine is completely replaced by talc±chlorite and fine-grained magnetite. Sample 07GNX37-1-1 in plane-polarized transmitted light.

magnesian tholeiitic basalt. The Keogh Lake picritic basalt forms both pillowed flows and minor sheet flows (Fig 10; cf. Greene et al., 2006, Fig 6). The sample of high-Mg pillow breccia taken close to the base of the hyaloclastite unit comes from a dark grey-green, massive layer of chaotically distributed, angular to subrounded, matrix-supported clasts (<35 cm), some of which exhibit chilled pillow margins, set in a chloritized and carbonate-altered clastic matrix.

Petrographically, the high-Mg pillow lavas contain abundant olivine, typically 10 to 25 vol% but reaching 40 vol% in some samples. Euhedral to subhedral olivine crystals (1–4 mm) are the sole phenocryst phase in high-Mg lavas with >12 wt% MgO (i.e., picrite, according to the revised IUGS classification discussed below). The morphology and abundance of olivine phenocrysts is similar in both high-Mg sheet flows associated with the pillow lavas (Fig 10) and the rare dikes that fed these lavas. The olivine in these rocks is predominantly replaced by talc, in contrast to the less magnesian olivine-bearing basalt, where replacement products generally include serpentine, chlorite, carbonate and quartz. Subequant to lath-shaped phenocrysts (<4 mm) of calcic plagioclase generally coexist with olivine in the latter group of lavas. Where olivine and plagioclase form glomerophytic intergrowths, olivine is the subordinate phase. Clinopyroxene in the high-Mg lavas is typically intergrown with calcic plagioclase to form subophitic to well-developed variolitic textures (illustrated by Greene et al., 2006, Fig 5).

GEOCHEMICAL CLASSIFICATION

Whole-rock analyses of Karmutsen basalt from northern Vancouver Island are plotted in Figure 11. All analyzed samples were examined petrographically to determine the degree of alteration, based on the abundance of amygdules infilled by secondary minerals, notably quartz, chlorite, carbonate, epidote, sericite, potassium feldspar, prehnite, zeolites and, rarely, pumpellyite; and the degree of replacement of calcic plagioclase, mainly by sericite and clay minerals but also involving partial replacement by chlorite, car-

bonate and epidote. Accordingly, the geochemical diagrams show only the least altered rocks, except for Figure 11D, where altered and amygdaloidal samples (>10 vol % amygdules) are represented.

A total alkalis versus silica (TAS) plot shows the subalkaline nature of the suite (Fig 11A). The lavas fall within the basalt field in the TAS classification (LeMaitre et al., 1989) and exhibit a large range of total alkali content (approx. 0.5–5.0 wt%) relative to their rather limited variation in silica (approx. 50 ± 2.5 wt%). The AFM diagram (Fig 11B) shows that the subalkaline basalts belong to a tholeiitic lineage with moderate iron enrichment.

Both least-altered and altered basalts are plotted in the IUGS classification scheme for high-Mg lavas (Fig 11C, D, respectively; Le Bas, 2000). Olivine-bearing basalt displays a considerable range of MgO abundances (approx. 5.5–19 wt%), extending from ‘normal’ basalt MgO concentrations through picrite to komatiitic compositions. The sampling is sufficient to illustrate a continuum of MgO abundances in these olivine-bearing lavas. The picrite in this classification scheme is defined by MgO >12 wt%, SiO₂ <52 wt% and Na₂O + K₂O <3 wt%. Komatiite has MgO >18 wt%, SiO₂ <52 wt%, total alkalis <2 wt% and TiO₂ <1 wt% (and see Greene et al., 2006, Fig 2C). Lavas that fall within the picrobasalt field in the high-Mg classification are, in fact, simply basalt in the TAS classification (Fig 11A) because, in order to qualify as ‘picrobasalt’, silica in these rocks must lie within the range 41 to 45 wt% SiO₂ (Le Bas, 2000), which is not the case. Olivine-free basalt falls near the lower limit of MgO concentrations (<7.5 wt%), but there is considerable compositional overlap between the olivine-free and olivine-bearing groups. Magnesium-poor lavas in the latter group are characterized by minor to trace amounts of olivine (Fig 11E).

The amygdaloidal and altered rocks plotted in Figure 11D show a distinct bias towards higher average alkali contents in the Mg-poor part of the compositional spectrum. The compositions of the least altered lavas likewise extend to similar high alkali abundances (Fig 11C). We conclude that this behaviour reflects varying degrees of alkali metasomatism unsuccessfully filtered by petrographic criteria alone.

Greene et al. (2006) observed that the Keogh Lake picritic basalt has the highest MgO abundances presently known within the Wrangellian flood basalt province, and that its primitive nature reflects partial melting generated by the ascent of a mantle plume beneath the oceanic plateau. It must be noted, however, that Karmutsen lavas with the highest MgO contents do not necessarily represent the compositions of such partial melts. For example, it is clear from the strong positive correlation between MgO and modal olivine (Fig 11E) that crystal sorting has played a role in determining the MgO content of these lavas. The high modal abundance of olivine in the most magnesian lavas may be reconciled by crystal accumulation, whereas compositions depleted in MgO likely reflect crystal fractionation of a more magnesian parental magma. It is important to note that rocks falling within the ‘komatiite’ field in the geochemical classification diagram contain approximately 40 vol% polyhedral olivine phenocrysts that are morphologically identical to those observed in the picrite and more magnesian basalt. These textural attributes, together with the complete lack of spinifex textures and close association with picritic basalt, are consistent with a cumulate origin for these MgO-rich compositions (cf. Kerr and

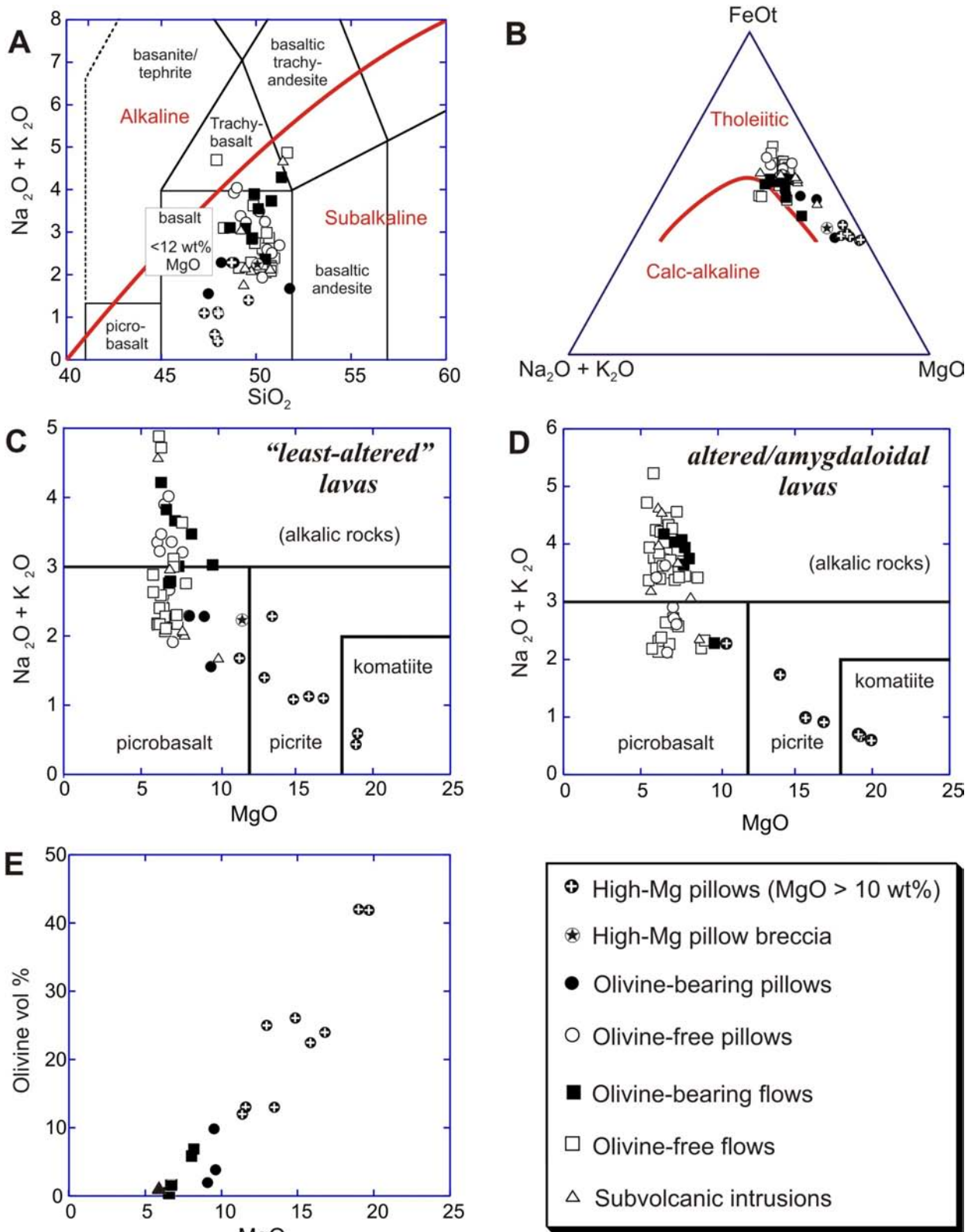


Figure 11. Whole-rock geochemical plots of Karmutsen basalts: A) total alkalis vs SiO_2 plot, showing the discriminant for alkaline and subalkaline rock series (Irvine and Baragar, 1971) and the IUGS classification of LeMaitre et al. (1989); B) total alkalis – total Fe as FeO (FeO_t) – MgO (AFM) plot, showing the discriminant between tholeiitic and calcalkaline rock series (Irvine and Baragar, 1971); C) and D) total alkalis vs MgO plots, showing the IUGS reclassification for high-Mg and picritic volcanic rocks (Le Bas, 2000); 'least altered' samples are shown in C, whereas altered and amygdaloidal samples are plotted in D; E) MgO vs modal olivine (vol%) plot for selected basalt samples. All analyses are recalculated to 100 wt% anhydrous with total iron as FeO.

Arndt, 2001). Thus, the most primitive melts in the Karmutsen Formation may have picritic rather than komatiitic compositions, which has relevance to potential models for Ni-Cu-PGE mineralization in the Wrangellian flood basalt province, as discussed below.

EVOLUTION OF THE OCEANIC PLATEAU

The stratigraphy of the Karmutsen Formation reflects the evolution of the Wrangellia oceanic plateau, a record of events not unlike modern hot-spot volcanoes such as Hawaii. The enormous outpourings of mainly aphyric pillow lava and localized sheet flows, represented by the basal pillow lava unit, mark the initial phase of submarine effusive activity, which constructed a seamount(s) rising from the deep ocean floor. The amygdaloidal nature of the uppermost pillow lavas and breccias in the overlying hyaloclastite unit indicate that, as the volcanic edifice grew and reached relatively shallow depths (<500 m), magmas were able to exsolve small amounts of volatiles. The eruption and emplacement of high-Mg lavas occurred at the transition from pillow lava emplacement to hyaloclastite deposition.

The thick sequence of volcanoclastic rocks deposited at the transition from submarine to subaerial volcanism likely reflects a variety of fragmentation processes, including thermal contraction of cooling pillows and internal expansion of growing pillow tubes, wave action, minor explosive activity triggered by volatile release and seawater-magma interaction, and earthquake-induced and gravitational collapse of oversteepened pillow ramparts. Many pillow-fragment breccias and sandstone horizons are rich in hyaloclastite material, presumably generated in shallow water and redeposited downslope by debris flows and turbidity currents, respectively.

As eruptions breached sea level, outpourings of highly amygdaloidal, fluid basaltic lava began to construct a gently sloping shield volcano. The plagioclase-phyric and megacrystic flows were emplaced late in the evolution of the shield. As volcanism waned due to decay of the mantle plume, thermal contraction of the lithosphere led to submergence of the shield. Localized deposition of intervolcanic limestone, pillow lava and hyaloclastite de-

posits intercalated with subaerial flows at the top of the Karmutsen succession records the final stages of effusive activity as submergence commenced. The presence of thin, discontinuous beds of basaltic sandstone and absence of a well-developed regolith or coarse conglomeratic deposits reflect the lack of deeply incised topography and rapid submergence. Cessation of volcanic activity led to the deposition of platform carbonate, represented by Quatsino limestone.

POTENTIAL FOR NI-CU-PGE MINERALIZATION

Flood basalt volcanism is associated with some important magmatic ore deposits, one premier example being the Ni-Cu-PGE sulphide mineralization of the Noril'sk-Talnakh region of Siberia (Fig 12). Economic concentrations of ore metals (production + reserves) at Noril'sk total some 555 million tonnes of 2.7% Ni, 3.9% Cu, 3 g/t Pt and 12 g/t Pd (Lightfoot and Hawkesworth, 1997). Naldrett (2004) noted that the Noril'sk ores exceed all other deposits, both Ni-Cu and PGE deposits, in the value of *in situ* metals per tonne. The sulphides are hosted by comagmatic intrusions that have been interpreted as conduits for part of a thick (~3.5 km) sequence of continental flood basalts erupted at the Permian-Triassic boundary. Like the Wrangellian flood basalts, the enormous volume of Siberian trap basalts (>2 x 10⁶ km³; Fedorenko, 1994) erupted over such a short time interval (250 ± 1 Ma; Sharma, 1997) that their consequently rapid eruption rate and lack of definitive evidence for emplacement during a major rifting event have been used to support a plume initiation model for their origin (cf. Greene et al., 2006). Aspects of the geology and genesis of the Noril'sk deposits and their related flood basalts, therefore, have metallogenic significance here.

Geochemical studies of the host intrusions and flood basalts at Noril'sk have indicated that, in a general sense (and albeit controversial), the processes that formed the ore deposits are to some degree reflected in the lavas (cf. Arndt et al., 2003; and *see* Naldrett, 2004 for a summary of pertinent controversies). The magmatic sulphides are hosted by gabbro-dolerite (9–16 wt% MgO) and olivine-rich picrite (18–29 wt% MgO) intrusions emplaced in Paleozoic sedi-

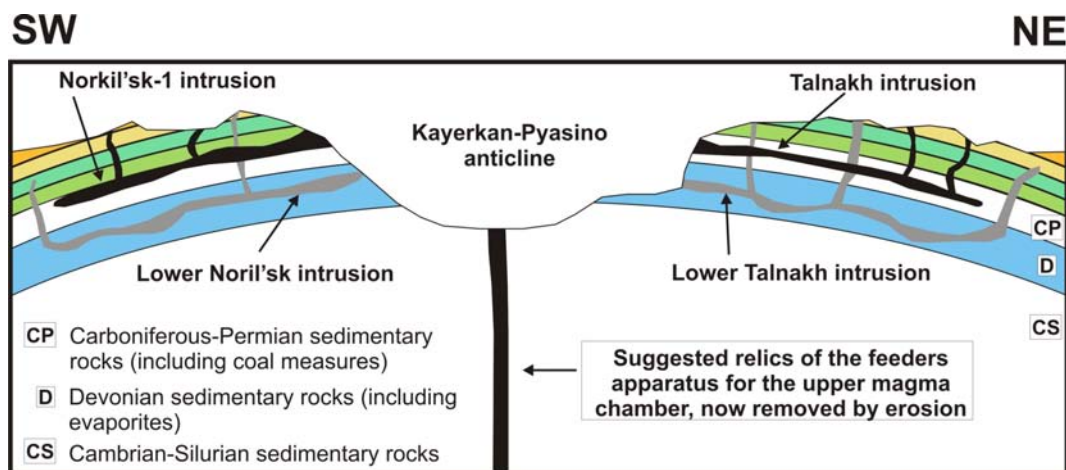


Figure 12. Schematic geological cross-section of the Noril'sk region (after Naldrett, 2004). Vertical scale is greatly exaggerated relative to horizontal scale.

mentary rocks that include sulphate-rich evaporites and coal measures. In order to satisfy the geochemical data, most workers agree that the complex architecture of conduits presently plugged by these intrusions were the sites of dynamic, open magmatic systems feeding the volcanic pile. Hot, primitive high-Mg (picritic) lavas form a small proportion of the overlying flood-basalt stratigraphy in the Noril'sk region (<1% of the stratigraphic thickness, according to Fedorenko, 1994), and are considered to represent parental magmas for the fractionated tholeiite. The presence of high-Mg lavas is nonetheless important, since these magmas inherently contain elevated abundances of Ni, and potentially Cu and PGE, and are the most likely candidates to be sulphur undersaturated and therefore capable of precipitating economic concentrations of metals in magmatic sulphides (Keays, 1995).

Some of the important evolutionary aspects of the Noril'sk-Talnakh system are shown schematically in Figure 13. Lightfoot and Hawkesworth (1997) observed that the chemical stratigraphy of the flood basalt pile records a strong depletion of chalcophile elements, as monitored by Cu, over approximately 200 m of stratigraphy, followed by

a gradual upward recovery in the tenor of Cu, Ni and PGE in the succeeding lavas over a 700 m stratigraphic interval. They emphasized that the lavas that show the strongest depletions of chalcophile elements, reflecting equilibration with sulphide ores at depth, are also those that have experienced the most crustal contamination by lower to midcrustal rocks. They argued that the increase in silica in contaminated magmas was primarily responsible for driving magmas towards sulphide ore formation in shallower crustal magma chambers, and not the addition of crust-derived S from evaporite-rich sediments. Since the sulphide ores contain an unusually high tenor of metals, the immiscible sulphide droplets must have scavenged metals from very large volumes of basaltic magma migrating through the conduit system, leaving the erupted lavas sympathetically depleted in these metals (the 'R factor' of Campbell and Naldrett, 1979). The gradual recovery in metal abundances exhibited by lavas higher in the stratigraphic section is considered to reflect progressive isolation of sulphides from dynamic interaction with fresh inputs of magma, possibly by gravitational settling of heavy sulphide droplets in hydrodynamic traps so as to form the more massive orebodies where Cu-rich ores subsequently fractionated

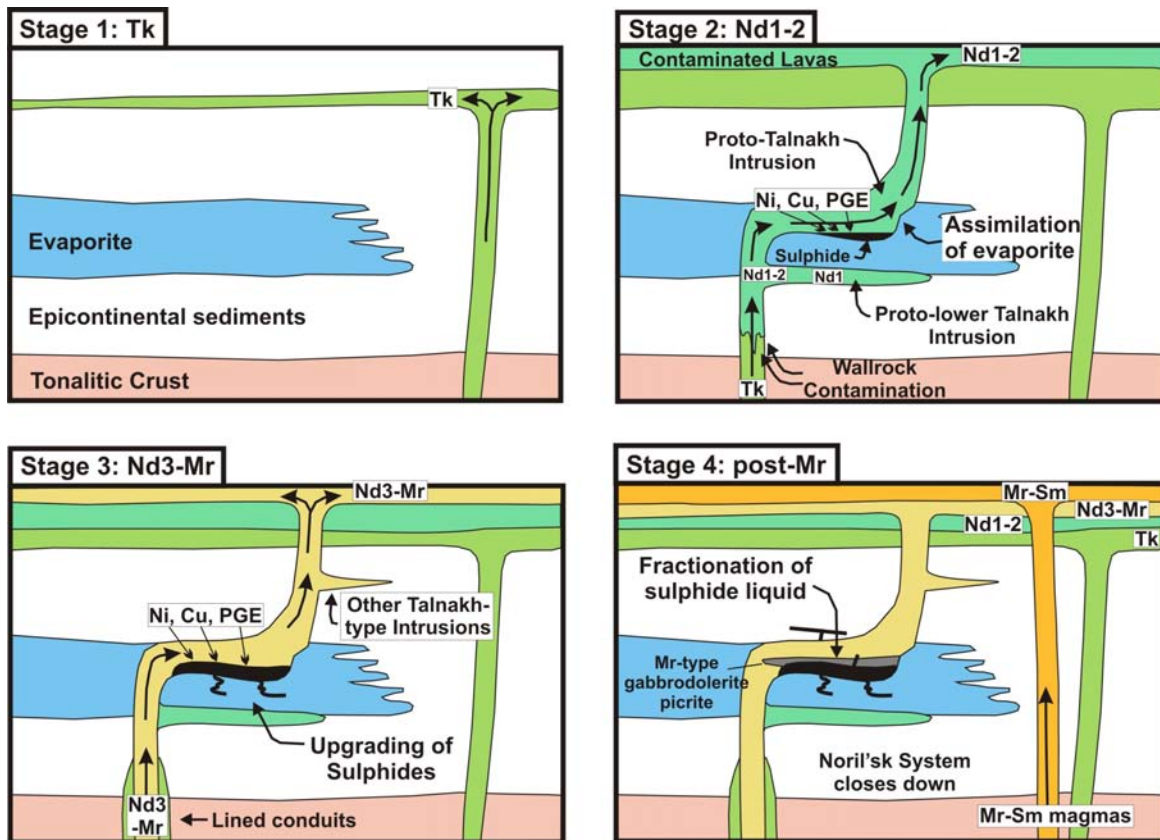


Figure 13. Schematic model for the evolution of the Noril'sk system (after Lightfoot and Hawkesworth, 1997). Stage 1: picritic and tholeiitic lavas of the Tuklonsky Formation (Tk) were erupted through conduits situated east of Noril'sk. Stage 2: Eruption of Nd1 lavas at Noril'sk generated by contamination and crystal fractionation of primitive Tk magmas with granodiorite at depth followed by assimilation of evaporitic sediments at shallow levels in the conduit system; the elevated silica and sulphur contents of contaminated magmas lead to precipitation of immiscible sulphides that ponded and reacted with fresh magma batches of Nd1 (Nadezhdinsky lavas) passing through the conduits. Stage 3: Continued throughput of Nd1 magma upgraded the Ni, Cu and PGE tenor of ponded sulphide liquids, causing the metal depletion observed in the lavas; as subsequent Nd2, Nd3 and Mr (Morongovsky) magmas ascended through the conduits, the sulphides became progressively isolated from the magmas and the degree of metal depletion declined, producing the observed upward increase of chalcophile element abundances with stratigraphic height. Stage 4: The Noril'sk system shut down as magmatism migrated northeast; sulphide liquids fractionated to form the Cu-rich ores.

(Czamanske et al., 1992; Lightfoot and Hawkesworth, 1997).

Exploration strategies for Ni-Cu-PGE deposits associated with the Wrangellian flood basalts should find certain aspects of the Noril'sk model intriguing. The occurrence of high-Mg basaltic lavas in the Karmutsen Formation of northern Vancouver Island demonstrates that this part of the flood basalt province received a supply of hot primitive magma, presumably S-undersaturated and therefore capable of forming magmatic sulphide ores. The lateral extent of these high-Mg lavas is presently unknown, and no systematic geochemical studies of the flood basalt stratigraphy have been undertaken with a view to prospecting for lavas with anomalously low chalcophile-element abundances.

Subvolcanic plumbing systems are exposed at the base of the Karmutsen Formation as dikes and sills in the Middle Triassic 'sediment-sill' unit (Muller et al., 1974, 'Daonella beds' of Fig 2). These pyritic shale and siltstone beds, and the older Paleozoic basement rocks they overlie, are potential sources of the siliceous and sulphur-bearing contaminants apparently required to induce magmatic sulphide segregation in primitive melts. As documented by Greene et al. (2006), small concentrations of disseminated sulphides have been observed at the contact of some subvolcanic Karmutsen sills; and some chemical subtypes of tholeiitic basalt with significant quantities of PGE appear to have erupted close to sulphur saturation (J.S. Scoates, unpublished data). These observations, together with the limited amount of geochemical data currently available for the Triassic flood basalts and their intrusive counterparts, should be particularly encouraging for mineral exploration.

ACKNOWLEDGMENTS

We wish to express our sincere thanks to Margaret Hanuse in Port McNeill and Dave Ross in the community of Holberg for graciously providing shelter from the storm; Kim Pilote for cheerfully dealing with truck and boat logistics; and Brian Grant for a field visit. We also thank Kathryn Gillis, Director of the School of Earth and Ocean Sciences at the University of Victoria, for providing access to point-counting equipment; and Tania Demchuk and Brian Grant for editorial logistics.

REFERENCES

- Armstrong, R.L., Muller, J.E., Harakal, J.E. and Muehlenbachs, K. (1985): The Neogene Alert Bay volcanic belt of northern Vancouver Island, Canada: descending-plate-edge volcanism in the arc-trench gap; *Journal of Volcanology and Geothermal Research*, Volume 26, pages 75–97.
- Arndt, N.T., Czamanske, G.K., Walker, R.J., Chauvel, C. and Fedorenko, V.A. (2003): Geochemistry and origin of the intrusive hosts of the Noril'sk-Talnakh Cu-Ni-PGE sulphide deposits; *Economic Geology*, Volume 98, pages 495–516.
- Campbell, I.H. and Naldrett, A.J. (1979): The influence of silicate:sulphide ratios on the geochemistry of magmatic sulphides; *Economic Geology*, Volume 74, pages 1503–1505.
- Carlisle, D. (1963): Pillow breccias and their aquagene tuffs, Quadra Island, British Columbia; *Journal of Geology*, Volume 71, pages 48–71.
- Carlisle, D. (1972): Late Paleozoic to mid-Triassic sedimentary-volcanic sequence on northeastern Vancouver Island; in Report of Activities, Part B, *Geological Survey of Canada*, Paper 72-1B, pages 24–30.
- Carlisle, D. and Suzuki, T. (1974): Emergent basalt and submergent carbonate-clastic sequences including the Upper Triassic Dilleri and Welleri zones on Vancouver Island; *Canadian Journal of Earth Sciences*, Volume 11, pages 254–279.
- Cas, R.A.F. and Wright, J.V. (1987): Volcanic Successions: Modern and Ancient; *Allen and Unwin*, London, United Kingdom, 528 pages.
- Czamanske, G.K., Kunilov, V.E., Zientek, M.L., Cabri, L.J., Likhachev, A.P., Calk, L.C. and Oscarson, R.L. (1992): A proton-microprobe study of magmatic sulphide ores from the Noril'sk-Talnakh district, Siberia; *The Canadian Mineralogist*, Volume 30, pages 249–287.
- DeBari, S.M., Anderson, R.G. and Mortensen, J.K. (1999) Correlation amongst lower to upper crustal components in an island arc: the Jurassic Bonanza arc, Vancouver Island, Canada; *Canadian Journal of Earth Sciences*, Volume 36, pages 1371–1413.
- Fedorenko, V.A. (1994): Evolution of magmatism as reflected in the volcanic sequence of the Noril'sk region; in Proceedings of the Sudbury-Noril'sk Symposium, Lightfoot, P.C. and Naldrett, A.J., Editors, *Ontario Geological Survey*, Special Volume 5, pages 171–184.
- Furin, S., Preto, N., Rigo, M., Roghi, G., Gianolla, P., Crowley, J.L. and Bowring, S.A. (2006): High-precision U-Pb zircon age from the Triassic of Italy: implications for the Triassic time scale and the Carnian origin of calcareous nannoplankton and dinosaurs; *Geology*, Volume 34, pages 1009–1012.
- Gamba, C.A. (1993): Stratigraphy and sedimentology of the Upper Jurassic to Lower Cretaceous Longarm Formation, Queen Charlotte Islands, British Columbia; in Current Research, Part A, *Geological Survey of Canada*, Paper 93-1A, pages 139–148.
- Gardner, M.C., Bergman, S.C., Cushing, G.W., MacKevett, E.M., Jr., Plafker, G., Campbell, R.B., Dodds, C.J., McClelland, W.C. and Mueller, P.A. (1988): Pennsylvanian pluton stitching of Wrangellia and the Alexander Terrane, Wrangell Mountains, Alaska; *Geology*, Volume 16, pages 967–971.
- Gradstein, F.M., Ogg, J.G. and Smith, A.G. (2004): A geologic time scale 2004; *Cambridge University Press*, Cambridge, United Kingdom, 610 pages.
- Greene, A.R., Scoates, J.S., Nixon, G.T. and Weis, D. (2006): Picritic lavas and basal sills in the Karmutsen flood basalt province, northern Vancouver Island; in Geological Fieldwork 2005, *BC Ministry of Energy, Mines and Petroleum Resources*, Paper 2006-1, pages 39–51.
- Greenwood H.J., Woodsworth, G.J., Read, P.B., Ghent, E.D. and Evenchick, C.A. (1991): Metamorphism; Chapter 16 in *Geology of the Cordilleran Orogen in Canada*, Gabrielse, H. and Yorath, C.J., editors, *Geological Survey of Canada*, Geology of Canada, Number 4, pages 533–570.
- Gunning, H.C. (1932): Preliminary report on the Nimpkish Lake quadrangle, Vancouver Island, British Columbia; *Geological Survey of Canada*, Summary Report, 1931, Part A, pages 22–35.
- Haggart, J.W. (1993): Latest Jurassic and Cretaceous paleogeography of the northern Insular Belt, British Columbia; in *Mesozoic Paleogeography of the Western United States*, Volume II, Book 71, Dunn, G. and McDougall, K., Editors, *Society of Economic Paleontologists and Mineralogists*, Pacific Section, pages 463–475.
- Haggart, J.W. and Carter, E.S. (1993): Cretaceous (Barremian–Aptian) radiolaria from Queen Charlotte Islands, British Columbia: newly recognized faunas and stratigraphic implications; in Current Research, Part E, *Geological Survey of Canada*, Paper 93-1E, pages 55–65.

- Irvine, T.N. and Baragar, W.R.A. (1971): A guide to the chemical classification of the common volcanic rocks; *Canadian Journal of Earth Sciences*, Volume 8, pages 523–548.
- Jeletzky, J.A. (1976): Mesozoic and ?Tertiary rocks of Quatsino Sound, Vancouver Island, British Columbia; *Geological Survey of Canada*, Bulletin 242, 243 pages.
- Jones, D.L., Silberling, N.J. and Hillhouse, J. (1977): Wrangellia — a displaced terrane in northwestern North America; *Canadian Journal of Earth Sciences*, Volume 14, pages 2565–2577.
- Keays, R.R. (1995): The role of komatiitic and picritic magmatism and S-saturation in the formation of ore deposits; *Lithos*, Volume 34, pages 1–18.
- Kerr, A.C. and Arndt, N.T. (2001): A note on the IUGS reclassification of the high-Mg and picritic volcanic rocks; *Journal of Petrology*, Volume 42, pages 2169–2171.
- Le Bas, M.J. (2000): IUGS reclassification of the high-Mg and picritic volcanic rocks; *Journal of Petrology*, Volume 41, pages 1467–1470.
- LeMaitre, R.W., Bateman, P., Dudek, A., Keller, J., Le Bas, M.J., Sabine, P.A., Schmid, R., Sorensen, H., Streckeisen, A., Wooley, A.R. and Zanettin, B. (1989): A classification of igneous rocks and glossary of terms; *Blackwell Scientific Publications*, Oxford, United Kingdom, 193 pages.
- Lewis, T.J., Lowe, C. and Hamilton, T.S. (1997): Continental signature of a ridge-trench-triple junction: northern Vancouver Island; *Journal of Geophysical Research*, Volume 102, pages 7767–7781.
- Lightfoot, P.C. and Hawkesworth, C.J. (1997): Flood basalts and magmatic Ni, Cu and PGE sulphide mineralization: comparative geochemistry of the Noril'sk (Siberian traps) and West Greenland sequences; in Large Igneous Provinces: Continental, Oceanic and Planetary Flood Volcanism, Mahoney, J.J. and Coffin, M.F., Editors, *American Geophysical Union*, Geophysical Monograph 100, pages 357–380.
- Massey, N.W.D. (1995a): Geology and mineral resources of the Alberni-Nanaimo lakes sheet, Vancouver Island, 92F/1W, 92F/2E and part of 92F/7E; *BC Ministry of Energy, Mines and Petroleum Resources*, Paper 1992-2, 132 pages.
- Massey, N.W.D. (1995b): Geology and mineral resources of the Cowichan Lake sheet, Vancouver Island, 92C/16; *BC Ministry of Energy, Mines and Petroleum Resources*, Paper 1992-3, 112 pages.
- Massey, N.W.D. (1995c): Geology and mineral resources of the Duncan sheet, Vancouver Island, 92B/13; *BC Ministry of Energy, Mines and Petroleum Resources*, Paper 1992-4, 112 pages.
- Massey, N.W.D., McIntyre, D.G., Desjardins, P.J. and Cooney, R.T. (2005): Digital geology map of British Columbia: whole province; *BC Ministry of Energy, Mines and Petroleum Resources*, GeoFile 2005-1.
- MINFILE (2007): MINFILE BC mineral deposits database; *BC Ministry of Energy, Mines and Petroleum Resources*, URL <<http://www.em.gov.bc.ca/Mining/GeolSurv/Minfile/>> [November 2007].
- Monger, J.W.H. and Journeay, J.M. (1994): Basement geology and tectonic evolution of the Vancouver region; in *Geology and Geological Hazards of the Vancouver Region*, Southwestern British Columbia, Monger, J.W.H., Editor, *Geological Survey of Canada*, Bulletin 481, pages 3–25.
- Monger, J.W.H., Price, R.A. and Tempelman-Kluit, D.J. (1982): Tectonic accretion and the origin of the two major metamorphic and plutonic belts in the Canadian Cordillera; *Geology*, Volume 10, pages 70–75.
- Muller, J.E. and Carson, D.J.T. (1969): Geology and mineral deposits of Alberni map-area, British Columbia (92F); *Geological Survey of Canada*, Paper 68-50, 52 pages.
- Muller, J.E., Northcote, K.E. and Carlisle, D. (1974): Geology and mineral deposits of Alert Bay – Cape Scott map-area, Vancouver Island, British Columbia; *Geological Survey of Canada*, Paper 74-8, 77 pages.
- Naldrett, A.J. (2004): Magmatic Sulphide Deposits: Geology, Geochemistry and Exploration; *Springer-Verlag*, Berlin, Germany, 727 pages.
- Nixon, G.T. and Orr, A.J. (2007): Recent revisions to the Early Mesozoic stratigraphy of northern Vancouver Island (NTS 102I; 092L) and metallogenic implications, British Columbia; in *Geological Fieldwork 2006*, *BC Ministry of Energy, Mines and Petroleum Resources*, Paper 2007-1, pages 163–177.
- Nixon, G.T., Kelman, M.C., Stevenson, D., Stokes, L.A. and Johnston, K.A. (2006a): Preliminary geology of the Nimpkish map area, northern Vancouver Island (92L/07); *BC Ministry of Energy, Mines and Petroleum Resources*, Open File 2006-5, scale 1:50 000.
- Nixon, G.T., Hammack, J.L., Koyanagi, V.M., Payie, G.J., Haggart, J.W., Orchard, M.J., Tozer, E.T., Friedman, R.M., Archibald D.A., Palfy, J. and Cordey, F. (2006b): Geology of the Quatsino – Port McNeill area, northern Vancouver Island; *BC Ministry of Energy, Mines and Petroleum Resources*, Geoscience Map 2006-2, scale 1:50 000.
- Nixon, G.T., Hammack, J.L., Koyanagi, V.M., Payie, G.J., Snyder, L.D., Panteleyev, A., Massey, N.W.D., Archibald D.A., Haggart, J.W., Orchard, M.J., Friedman, R.M., Tozer, E.T., Tipper, H.W., Poulton, T.P., Palfy, J., Cordey, F. and Barron, D.J. (2006c): Geology of the Holberg – Winter Harbour area, northern Vancouver Island; *BC Ministry of Energy, Mines and Petroleum Resources*, Geoscience Map 2006-3, scale 1:50 000.
- Nixon, G.T., Snyder, L.D., Payie, G.J., Long, S., Finnie, A., Friedman, R.M., Archibald D.A., Orchard, M.J., Tozer, E.T., Poulton, T.P. and Haggart, J.W. (2006d): Geology of the Alice Lake area, northern Vancouver Island; *BC Ministry of Energy, Mines and Petroleum Resources*, Geoscience Map 2006-1, scale 1:50 000.
- Northcote, K.E. and Muller, J.E. (1972): Volcanism, plutonism, and mineralization: Vancouver Island; *Canadian Institute of Mining, Metallurgy and Petroleum*, Bulletin 65, pages 49–57.
- Richards, M.A., Jones, D.L., Duncan, R.A. and DePaolo, D.J. (1991): A mantle plume initiation model for the Wrangellia flood basalt and other oceanic plateaus; *Science*, Volume 254, pages 263–267.
- Riddihough, R.P. and Hyndman, R.D. (1991): Modern plate tectonic regime of the continental margin of western Canada; in *Geology of the Cordilleran Orogen in Canada*, Gabrielse, H. and Yorath, C.J., Editors, *Geological Survey of Canada*, Geology of Canada, Number 4, pages 435–455.
- Sharma, M. (1997): Siberian traps; in Large Igneous Provinces: Continental, Oceanic and Planetary Flood Volcanism, Mahoney, J.J. and Coffin, M.F., Editors, *American Geophysical Union*, Geophysical Monograph 100, pages 273–295.
- Sutherland Brown, A. (1968): Queen Charlotte Islands; *BC Ministry of Energy, Mines and Petroleum Resources*, Bulletin 54, 226 pages.
- van der Heyden, P. (1991): A Middle Jurassic to Early Tertiary Andean-Sierran arc model for the Coast Belt of British Columbia; *Tectonics*, Volume 11, pages 82–97.
- Wheeler, J.O. and McFeely, P. (1991): Tectonic assemblage map of the Canadian Cordillera and adjacent parts of the United States of America; *Geological Survey of Canada*, Map 1712A, scale 1:2 000 000.
- Yorath, C.J., Sutherland Brown, A. and Massey, N.W.D. (1999): LITHOPROBE, southern Vancouver Island: geology; *Geological Survey of Canada*, Bulletin 498, 145 pages.